energies

MDPI

Article

A Detection Method for Slight Inter-Turn Short-Circuit Fault in Dry-Type Air-Core Shunt Reactors

Jie Wu [1,2], Wei Zhen [1,2], Zhengwei Chang [1,2], Man Zhang [3,*], Yumin Peng [3], Ying Liu [3] and Qi Huang [3]

[1] Electric Power Research Institute of State Grid Sichuan Electric Power Company, Chengdu 610041, China
[2] Power Internet of Things Key Laboratory of Sichuan Province, Chengdu 610041, China
[3] School of Mechanical and Electrical Engineering, University of Electronic Science and Technology of China, Chengdu 610059, China; hwong@uestc.edu.cn (Q.H.)
* Correspondence: zhangman@uestc.edu.cn

Abstract: Dry-type air-core shunt reactors are integral components in power transmission and distribution networks, designed to control reactive power and enhance system stability. However, inter-turn short-circuit faults (ISCFs) are common occurrences in shunt reactors, which are caused by various factors, including manufacturing defects, insulation degradation, or operational stresses. At the early stage of the ISCFs, the current does not reach a sufficient level to activate the protective equipment. These faults may lead to serious consequences, such as overheating, insulation breakdown, and even catastrophic failures, posing risks to the entire power system. Therefore, developing an effective and reliable detection method for ISCFs at the early stage is paramount. In this paper, a new method named the fault detection factor (FDF) based on equivalent resistance is presented to detect the slight ISCFs in dry-type air-core shunt reactors considering insulation resistance. In addition, the effect of noise signal existence in the monitoring process is taken into account. A moving average filter is adopted to guarantee both the sensitivity and the reliability of the proposed method. Ultimately, the simulation results of the FDF under different conditions are presented, which show the effectiveness and potential of the proposed method in observing and monitoring slight ISCFs.

Keywords: dry-type air-core shunt reactors; inter-turn short-circuit fault; equivalent resistance; high sensitivity

Citation: Wu, J.; Zhen, W.; Chang, Z.; Zhang, M.; Peng, Y.; Liu, Y.; Huang, Q. A Detection Method for Slight Inter-Turn Short-Circuit Fault in Dry-Type Air-Core Shunt Reactors. *Energies* **2024**, *17*, 1709. https://doi.org/10.3390/en17071709

Academic Editor: Daniel Morinigo-Sotelo

Received: 7 January 2024
Revised: 26 February 2024
Accepted: 4 March 2024
Published: 3 April 2024

1. Introduction

The dry-type air-core reactor has advantages such as simple structure, good linearity, and easy maintenance. It is widely used in power systems for reactive power compensation and system voltage stabilization [1,2]. However, due to manufacturing defects, mechanical damage, material aging, and arc breakdown, the reactor is prone to frequent failures [3,4]. Among various common faults, inter-turn short-circuit faults (ISCFs) account for the largest proportion [5]. At the early stage of inter-turn short-circuit faults, the number of short-circuited turns is small, and the current change in the reactor is small, causing overcurrent protection to fail. However, when the internal circulating current between the coil turns due to the inter-turn short circuit is too large, it can lead to excessively high local temperatures in the coil, further damaging the inter-turn insulation. This, in turn, leads to more coil turns near the short-circuit point experiencing short-circuit faults [6]. In severe cases, the local high temperature generated by the short-circuit current will burn out the reactor, or even cause a combustion accident, affecting the safe and stable operation of the power system. Therefore, a highly sensitive detection method for ISCFs in dry-type air-core reactors is of great significance for their stable operation.

The existing monitoring methods for inter-turn short-circuit faults in dry-type air-core reactors mainly include the magnetic field monitoring method [7,8], temperature monitoring method [9,10], vibration monitoring method [11,12], and electrical quantity monitoring method using measured voltage and current.

In detail, an online detection algorithm for turn-to-turn faults in iron core reactors was proposed in [7], utilizing additional sensor coils to measure the leakage magnetic field. A method for detecting ISCFs based on the spatial magnetic field distribution of dry-type air-core reactors was proposed in [8]. This involved establishing functions using a curve-fitting method to assess the degree of fault. However, the magnetic field monitoring method requires the installation of induction coils at both ends of the reactor, it is complicated, and the additional equipment can affect the normal operation of the reactor [13]. As for the temperature monitoring method, [9] designed a system to monitor the condition of a reactor, where several wireless temperature sensors were installed at the node needed to measure the temperature. A new method for fitting the temperature field with a multi-component normal distribution was proposed using temperature collected with an RFID chip [10]. The measured temperature was then compared with the ideal temperature to obtain the operating state of the reactor. Nevertheless, at the early stages of ISCF, temperature rise is relatively slow, and environmental factors have a significant impact on temperature rise. Therefore, the sensitivity of the temperature monitoring method is low, and it cannot promptly detect faults [14]. The vibration signal from an outer encapsulation of a reactor was utilized for ISCF detection in [11]. Extracted features from the vibration signal were employed to train a classification model. The identification and localization of ISCF rely on detecting alterations in the vibration distribution characteristics on the surface of the reactor in [12]; both methods in [11,12] require a laser Doppler vibrometer to measure the vibration velocity of the reactor. A hierarchical neural network method was suggested for locating inter-turn faults in [15]. This approach necessitated additional temperature sensors and humidity sensors, as well as current and voltage sensors, depending on the number of monitoring areas.

As for the electrical quantity monitoring method, the monitoring of ISCFs was suggested through the resonance frequency shift of input impedance in [16]. An online detection method for ISCFs of a shunt reactor utilizing an analysis grounded in impulse coupling injection was introduced in [17,18], where the fault can be detected by monitoring the frequency response characteristics of the injected pulse signal. However, additional equipment to generate pulse signals is required. A monitoring method based on impedance variation was proposed in [19,20]. A technique was introduced in [21] for monitoring ISCFs in dry-type air-core reactors based on current distribution characteristics under multiple-harmonic excitation. Ref. [22] presented a model simulating inter-turn faults in shunt reactors with an electric circuit and introduced three algorithms—zero-sequence reactance, negative-sequence reactance, and phase impedance—to detect inter-turn faults. Ref. [23] introduced an online device for monitoring reactor short-circuit faults based on the power angle. In the realm of techniques employing electrical parameters, many simulations and experiments focus on scenarios where one or a few turns of the reactor coil are entirely shorted. This often overlooks the insulation resistance between turns when an ISCF happens, a crucial factor that significantly impacts the detection algorithm, especially when only a portion of the coil is locally shorted rather than the entire turn. At the initial stage of an ISCF, the insulation material between coil turns is not completely damaged, and the short-circuited coil turns only have partial contact. Therefore, there exists insulation resistance [24–26].

At the early stage of an ISCF, due to the relatively small number of short-circuited turns, the electrical parameters of the reactor, such as current, equivalent inductance, and equivalent impedance, do not show significant changes. However, the increase in equivalent resistance and active power is relatively noticeable [27–30]. Therefore, this paper starts from the change patterns of equivalent resistance and active power at the early stage of an ISCF in dry-type air-core reactors. It selects appropriate electrical quantities for detection and proposes corresponding online monitoring methods. The transition from the local short circuit to the global short circuit of coil turns is an accumulating process, during which the insulation resistance is in a dynamically changing state. Therefore, the magnitude of insulation resistance affects the effectiveness of fault detection methods. The

adaptability of the proposed online detection method is verified through simulation under different insulation resistance values.

In this paper, finite element analysis is used to simulate and calculate the electrical parameters of the reactor when an ISCF occurs at different positions. At first, the position with the least noticeable change in electrical parameters during the fault is determined without considering insulation resistance. Based on this, the variation patterns in equivalent resistance and active power with respect to insulation resistance are analyzed when the ISCF occurs at this position. Then, an exponential function based on equivalent resistance is constructed to achieve online detection of slight ISCFs in dry-type air-core reactors. Furthermore, this paper analyzes and discuss the influence of noise signals on the sensitivity and reliability of the proposed method. As this paper aims to propose a highly sensitive online fault detection method for the early stages of ISCFs in dry-type air-core reactors, all analyses and calculations in this paper are conducted under the condition that only one-turn of the coil is shorted.

2. Materials and Methods

2.1. Equivalent Circuit

A dry-type air-core reactor usually consists of multiple encapsulates, and each encapsulate composes of multiple coils connected parallel. The equivalent circuit when an inter-turn short-circuit fault (ISCF) occurs at the n^{th} coil is shown in Figure 1. In the figure, I_i, R_i, and L_i represent the branch current, resistance, and self-inductance of the i^{th} coil, respectively; I_{n+1}, R_{n+1}, and L_{n+1} represent the induced current, resistance, and self-inductance of the short-circuit loop, respectively; R_f represents the insulation resistance; M_{ij} represents the mutual inductance between the i^{th} and j^{th} coils; $M_{i(\text{n+1})}$ represents the mutual inductance between the i^{th} coil and the short-circuit loop; I represents the bus current; and U represents the terminal voltage.

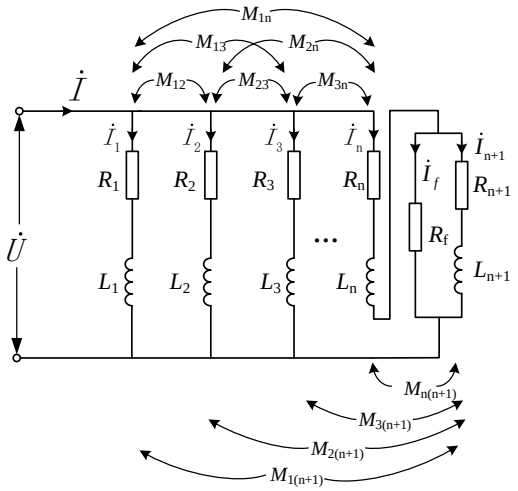

Figure 1. The equivalent circuit for inter-turn short-circuit faults of dry-type air-core reactors.

The condition under which an ISCF occurs and $R_f \neq 0$ is defined as a local ISCF; otherwise, it is defined as a global ISCF when $R_f = 0$. Therefore, the following equation can be obtained based on the Kirchhoff Voltage Law (KVL):

$$(\boldsymbol{R} + j\omega\boldsymbol{M})\boldsymbol{I} = \boldsymbol{U} \tag{1}$$

where

$$\boldsymbol{R} = \text{diag}(R_1, R_2, \cdots, R_\text{n} + R_\text{f}, R_{\text{n}+1} + R_\text{f}) \tag{2}$$

$$\boldsymbol{M} = \begin{bmatrix} L_1 & M_{12} & \cdots & M_{1n} & M_{1(n+1)} \\ M_{21} & L_2 & \cdots & M_{2n} & M_{2(n+1)} \\ \vdots & \vdots & \ddots & \vdots & \vdots \\ M_{n1} & M_{n2} & \cdots & L_n & M_{n(n+1)} \\ M_{(n+1)1} & M_{(n+1)2} & \cdots & M_{(n+1)n} & L_{n+1} \end{bmatrix} \tag{3}$$

$$\boldsymbol{I} = [I_1, I_2, \cdots, I_n, I_{n+1}]^T \tag{4}$$

$$\boldsymbol{U} = [U_1, U_2, \cdots, U_n, U_{n+1}]^T \tag{5}$$

where $U_{n+1} = 0$, which is the voltage of the shorted turn.

2.2. Inter-Turn Short-Circuit Fault When $R_f = 0$

After a global ISCF occurs in a dry-type air-core reactor, the bus current and equivalent inductance only change a little, while the equivalent resistance and active power increase more obviously [27–30]. Therefore, in this paper, the equivalent resistance and active power of the dry-type air-core reactor are selected for analysis.

The layers of the reactor are denoted as the 1st encapsulate, 2nd encapsulate... and 13th encapsulate, from the innermost to the outermost encapsulate. Since the dry-type air-core reactor is axially symmetric, only the upper half section is considered for ISCFs. The reactor is divided into 10 equal segments along the height, and a point is selected at every 1/10 segment interval from the symmetrical position upwards as the fault height, and 5 different fault positions are chosen to be investigated along the axial direction. The distribution of fault heights is shown in Figure 2.

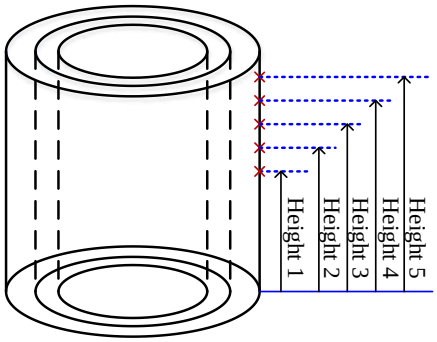

Figure 2. The distribution of fault height.

2.2.1. ISCF Occurring in Different Coils within the Same Encapsulate

This paper takes a BKDCKL—20000/35 dry-type air-core reactor as an example, whose specific parameters are shown in Table 1. Based on its geometric parameters and material properties, a finite element simulation model is constructed for simulation calculations. Through post-processing, equivalent circuit parameters (equivalent resistance, equivalent reactance, and busbar current) during normal and fault operations of the reactor can be obtained. This enables the determination of the active power consumed during the operation of the reactor.

Table 1. The reactor parameters.

Parameters	Value	Parameters	Value
Rated capacity (kVar)	20,000	Rated current (A)	989.7
Rated voltage (kV)	20.21	Height (mm)	1990
Number of encapsulates	13	Outer radius (mm)	2807.1
Number of coils	44	Equivalent reactance (Ω)	20.42
Rated frequency (Hz)	50	Equivalent resistance (Ω)	0.051

Since there is more than one coil in each encapsulate, it is necessary to investigate the difference in the referred electrical parameters among coils in the same encapsulate. Thus, some simulations are carried out with finite element analysis (FEA). Due to the axial symmetry of the physical model, the reactor is reduced to a 1/2 model to simplify the analysis of the electromagnetic field within it. To compute the equivalent resistance and active power, the bus current is required. A combination of 2D FEA and an electric circuit is employed to calculate the bus current. An AC voltage source is applied to the electric circuit, connected in series with the reactor. The coils within each encapsulate are connected in parallel within the electric circuit. In addition, the infinite element domain boundary is adopted to simulate the infinitely extended region around the reactor. Therefore, the equivalent resistance and active power variation can be computed when the global ISCF occurs and one turn of the coil is shorted at height 1 in the 1st, 3rd, and 11th encapsulates of the dry-type air-core reactor. The variation in equivalent resistance and active power is calculated, which is defined as the ratio of amplitude under the ISCF to this under normal conditions; the results are shown in Table 1. As shown in Table 2, the equivalent resistance and active power ratio for different coils are almost the same when the global ISCF occurs at the same height in the same encapsulate. Therefore, the subsequent simulation results and analyses in this paper only consider the scenario where the ISCF occurs in the first coil within each encapsulate.

Table 2. The ratio of variables for a global inter-turn short-circuit fault at each winding at Height 1.

Encapsulate	Coil	Equivalent Resistance Ratio	Active Power Ratio
1	1	15.982	16.176
	2	16.117	16.317
	3	16.260	16.463
	4	16.394	16.600
	5	16.535	16.744
3	1	26.506	27.299
	2	26.693	27.499
	3	26.878	27.695
	4	27.077	27.905
11	1	53.580	60.194
	2	53.485	60.078
	3	53.420	59.988

2.2.2. ISCF Occurring in Different Encapsulates

The equivalent resistance ratio and the active power ratio of normal operation to ISCFs occurring at different heights of the 1st coil of each encapsulation are shown in Figures 3 and 4, respectively. As observed in the figures, both the equivalent resistance and active power of the reactor exhibit an initial increase followed by a decrease as the faulted encapsulate moves outward. The equivalent resistance and active power experience significant increments in the presence of an ISCF, reaching up to 50 and 60 times the rated values, respectively, without accounting for insulation resistance. Conversely, they decrease as the fault height approaches the end. The closer to the end, the less noticeable the changes in the investigated equivalent parameters. It can be seen that the changes in equivalent resistance and active power are minimal when the ISCF occurs at Height 5 in the 1st encapsulate. Therefore, this position is selected for further fault simulation analysis.

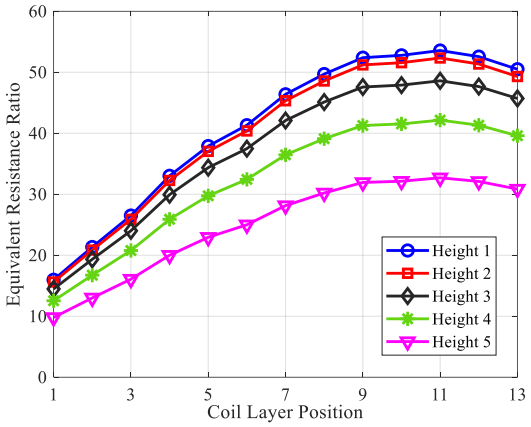

Figure 3. The equivalent resistance ratio variation for a global inter-turn short-circuit fault.

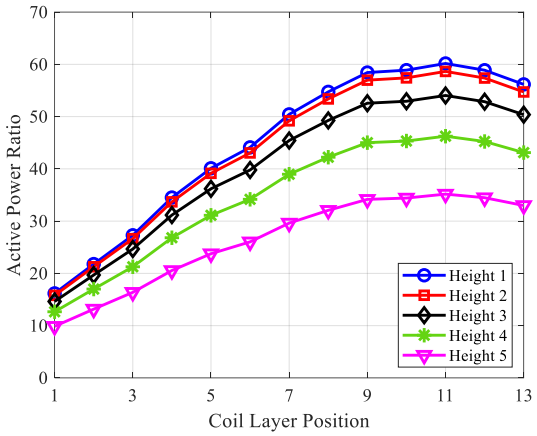

Figure 4. The active power ratio variation for a global inter-turn short-circuit fault.

2.3. Local Inter-Turn Short-Circuit Fault When $R_f \neq 0$

2.3.1. ISCF Detection Method

The authors of [26] proposed a highly sensitive ISCF detection method that takes insulation resistance into account. It determines the operational status of the reactor by using the amplitude of the power loss factor (*PLF*) during a fault. The calculation of *PLF* is shown in (6)

$$PLF = \frac{1}{2}\left[\left(\frac{P_{\text{act}}^{\text{ac}}}{P_{\text{N}}^{\text{ac}}}\right)^2 + \left(\frac{R_{\text{act}}}{R_{\text{N}}}\right)^2\right] \tag{6}$$

where $P_{\text{act}}^{\text{ac}}$ and P_{N}^{ac} are the active power under an ISCF and under normal conditions, respectively, and R_{act} and R_{N} are the equivalent resistance under an ISCF and under normal conditions, respectively.

The bus current under an ISCF and under normal conditions is defined as I_{sc} and I_{N}, respectively. Then the active power under an ISCF and under normal conditions can be expressed as

$$P_{\text{act}}^{\text{ac}} = I_{\text{sc}}^2 R_{\text{act}}, \tag{7}$$

$$P_{\text{N}}^{\text{ac}} = I_{\text{N}}^2 R_{\text{N}}, \tag{8}$$

The investigated reactor consists of 44 coils in parallel, which is composed of hundreds of turns. Therefore, the amplitude of the bus current remains almost unchanged under an

ISCF, it makes $\frac{I_{sc}}{I_N} \approx 1$. Therefore, *PLF* can be approximated as (9), which is approximately equal to $\left(\frac{R_{act}}{R_N}\right)^2$, denoted as PLF_A in (10).

$$PLF = \frac{1}{2}\left[\left(\frac{P_{act}^{ac}}{P_N^{ac}}\right)^2 + \left(\frac{R_{act}}{R_N}\right)^2\right] = \frac{1}{2}\left[\left(\frac{I_{sc}}{I_N}\right)^4 + 1\right]\left(\frac{R_{act}}{R_N}\right)^2 \approx \left(\frac{R_{act}}{R_N}\right)^2 \tag{9}$$

$$PLF_A = \left(\frac{R_{act}}{R_N}\right)^2 \tag{10}$$

According to (9) and (10), it can be observed that when the reactor is operating normally, both *PLF* and PLF_A are equal to 1. However, after an ISCF occurs in the reactor, the equivalent resistance increases, causing both parameters to be greater than 1. Therefore, the operational status of the reactor can be determined based on the amplitudes of these parameters.

Different insulation resistance values ($R_f = 0.1 \sim 100\ \Omega$) were set at Height 5 in the 1st encapsulate. Simulations were conducted to simulate a local ISCF under different degrees of insulation damage. The variation curves of the equivalent resistance ratio, active power ratio, *PLF*, and PLF_A at different insulation resistances are shown in Figure 5. As shown in the figure, with the development of the fault, as the insulation resistance decreases, all four parameters increase. The curves of the equivalent resistance change ratio and the active power change ratio overlap. *PLF* and PLF_A are essentially equal, and both are greater than the other two parameters, indicating higher sensitivity. However, at the early stages of the fault, when the insulation resistance $R_f > 40\ \Omega$, the amplitudes of the above parameters tend to stabilize (equivalent resistance ratio ≈ active power ratio ≈ 1.028, $PLF \approx PLF_A \approx 1.055$). With an increase in insulation resistance, there is no significant change. Therefore, it can be concluded that if an ISCF occurs at a height closer to the end of the winding, at the early stages of insulation damage ($R_f > 40\ \Omega$), the amplitudes of the above parameters tend to approach 1, which may lead to misjudgment. Therefore, based on *PLF*, this paper proposes a higher sensitivity method for ISCF detection in reactors.

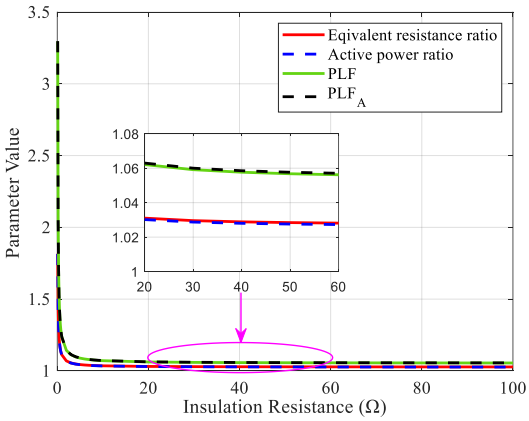

Figure 5. The curve of parameter variation with insulation resistance.

Replacing the exponent of the PLF_A with variable a yields the fault detection factor (*FDF*). The expression for the *FDF* is given by (11),

$$FDF = \left(\frac{R_{sc}}{R_N}\right)^a = \left[1 + \frac{R_{sc} - R_N}{R_N}\right]^a = (1 + X_R)^a \tag{11}$$

where $X_R = \frac{R_{sc} - R_N}{R_N}$.

Expanding (11) using the Taylor series can be expressed as (12),

$$\begin{aligned} FDF = \quad & 1 + aX_{\mathrm{R}} + \tfrac{a(a-1)}{2!}X_{\mathrm{R}}^2 + \cdots \\ & + \tfrac{a(a-1)\cdots(a-n+1)}{n!}X_{\mathrm{R}}^n + o\left(X_{\mathrm{R}}^n\right) \end{aligned} \tag{12}$$

According to (12), the value of the *FDF* increases with the increment in a with the same X_{R}. The results of the *FDF* varying with different insulation resistance, including $R_f = 20\,\Omega, 40\,\Omega$, and $60\,\Omega$, are shown in Figure 6. It can be seen that the sensitivity of the *FDF* to the local ISCF can be improved by increasing the value of a.

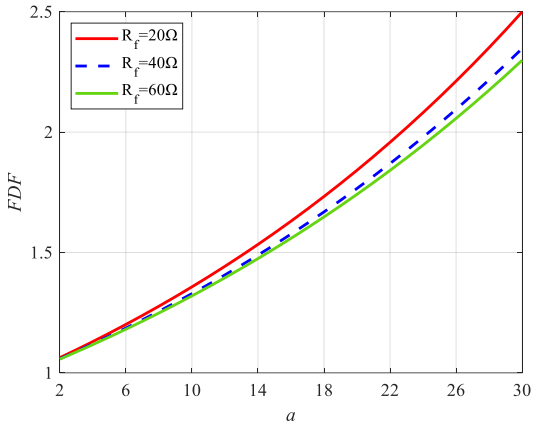

Figure 6. The fault factor curve with a.

Ref. [23] proposed a method to detect ISCFs using the power angle. When the insulation resistance $R_f = 60\,\Omega$, the power angle of the investigated reactor is 1.5687 rad, while the power angle is 1.5688 rad when the reactor works normally. Thus, it is hard to distinguish between the fault and normal conditions when the insulation resistance is considered. A monitoring method based on impedance variation was proposed in [20], and it presented that the equivalent resistance change was more obvious than the equivalent reactance when an ISCF happened. However, the equivalent resistance only increased by 2.7% at the early stage of ISCF ($R_f = 60\,\Omega$) for the investigated reactor. According to the results in Figure 6, the proposed method has better sensitivity with a bigger exponent 'a'.

2.3.2. The Impact of Noise Signals on Fault Detection Reliability

However, in the process of monitoring the reactor's condition, the real-time collection of its voltage and current signals is necessary to calculate the reactor's equivalent resistance during operation. The analog signals collected by voltage and current transformers require further processing through signal conditioning circuits and AD converters to be converted into digital signals, which are then sent to the host computer for calculation. Inevitably, this process introduces noise signals, affecting the reliability of the detection method.

To mimic real-world conditions, white noise is introduced into the simulated data of the reactor fault. The relationship between the reliability of the detection scheme and the parameter 'a' is discussed. Since the corresponding fault factor also fluctuates within a small range when the reactor is operating normally, a threshold value ΔF is set. When $FDF - 1 > \Delta F$, it indicates an inter-turn short-circuit fault in the reactor operation. Conversely, it indicates normal operation. In the event of an inter-turn short circuit, a significant change in the corresponding fault factor is expected to aid in fault discrimination.

Under simulated normal operating conditions, the variation in the fault factor is shown in Figure 7 for different values of the exponent 'a' ($a = 2 \sim 10$). Setting the fault at Height 5 in the first layer encapsulate and letting $R_{\mathrm{f}} = 100\,\Omega$, the variation in the fault factor for different values of the exponent 'a' in the fault state is shown in Figure 8.

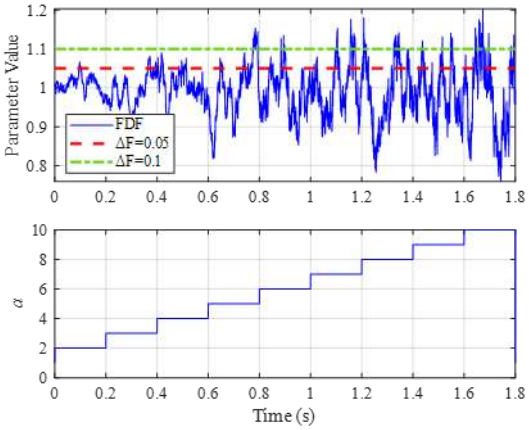

Figure 7. The fault factor curve with the variation in exponent a when the reactor is under normal conditions.

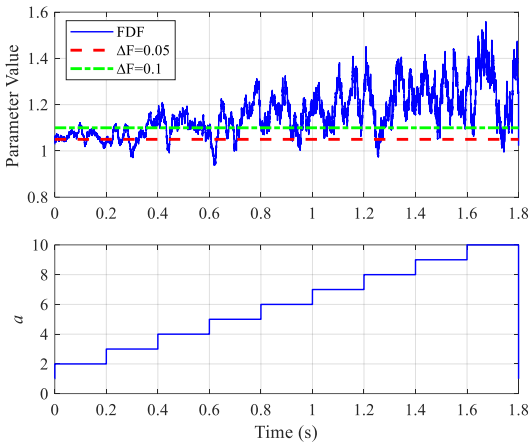

Figure 8. The fault factor curve with the variation in exponent a when the reactor is under an inter-turn short-circuit fault condition.

Due to the presence of noise signals, as the value of 'a' increases, the fluctuation amplitude of the fault factor *FDF* during the normal operation of the reactor also increases. When the threshold value is set to $\Delta F = 0.05$, there are intervals in the range of 'a' from 2 to 10 where the threshold is exceeded, indicating a possibility of misjudgment as a fault operation. When $\Delta F = 0.1$, intervals exceeding the threshold begin to appear at $a = 5$. Additionally, the likelihood of misjudgment increases with an increase in 'a'.

Correspondingly, during the operation of the reactor with an inter-turn short-circuit fault, there is a possibility of misjudging it as normal operation within the range of 'a' from 2 to 10. Although the fluctuation amplitude of the *FDF* during reactor fault operation increases with an increase in 'a', the average value also shifts upwards, thereby reducing the likelihood of misjudgment.

From the aforementioned analysis of two reactors, it can be concluded that considering noise in the signal, as 'a' increases, there is an increased likelihood of normal operation being mistakenly identified as a fault, while the likelihood of a fault being mistakenly identified as normal operation decreases.

3. Results

To ensure the reliability of fault detection while improving the sensitivity of the fault factor, this paper proposes applying a moving average filter (MAF) to the calculated *FDF*.

This is performed to reduce data fluctuations caused by noise signals, thereby minimizing misjudgments. The expression for MAF is given by (13).

$$x_t = \frac{1}{N}\sum_{i=0}^{N-1} x_{t-i}, \tag{13}$$

where x_t is the value of the time series at time t and N is the order of the MAF, representing the number of data points included in the averaging window.

The simulation results with the MAF applied are shown in Figures 9 and 10. After filtering, when the threshold values $\Delta F = 0.05$ and $\Delta F = 0.1$, within the range of 'a' from 2 to 10, the fault factor $FDF - 1$ under normal conditions is less than ΔF. This enables the correct determination of the reactor's operational status. During the operation of the reactor with an inter-turn short-circuit fault, when the threshold value is $\Delta F = 0.05$, the correct determination of the reactor's operational status is possible after a ≥ 4. When $\Delta F = 0.1$, correct determination is possible after $a \geq 6$. Additionally, with an increase in 'a', the FDF during a fault operation deviates further from the FDF during normal operation. Consequently, it becomes easier to determine the operational status of the reactor.

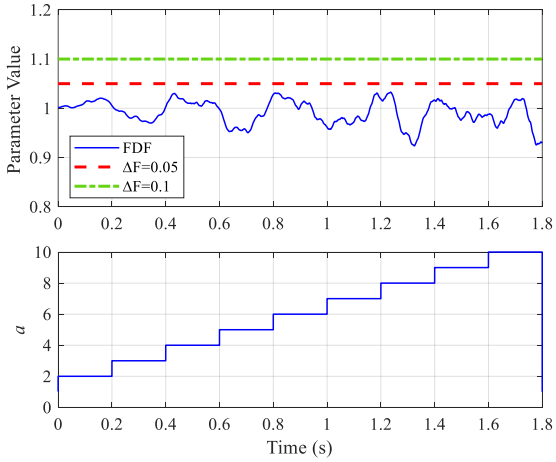

Figure 9. The fault factor curve handled by a moving average filter with the variation in exponent a when the reactor is under normal conditions.

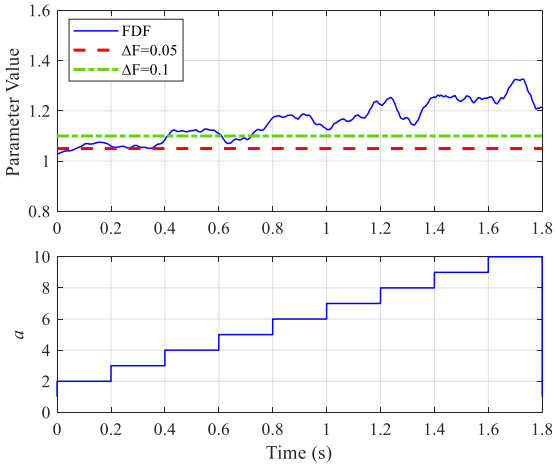

Figure 10. The fault factor curve handled by a moving average filter with the variation in exponent a when the reactor is under an inter-turn short circuit-fault condition.

To verify the effectiveness of the proposed method further, another reactor BKGKL-20000/35 (namely, reactor II) is also simulated, whose specific parameters are shown in Table 3. Under the simulated normal operating conditions, the variation in the fault factor

is shown in Figure 11 for different values of the exponent 'a' (a = 2~10). Letting $R_f = 100\ \Omega$, the variation in the fault factor for different values of the exponent 'a' in the fault state is shown in Figure 12. A similar conclusion can be obtained as follows: when the threshold value is $\Delta F = 0.05$ and $\Delta F = 0.1$, within the range of '*a*' from 2 to 10, the fault factor $FDF - 1$ under normal conditions is less than ΔF. This enables the correct determination of the reactor's operational status. During the operation of the reactor with an inter-turn short-circuit fault, when the threshold value is $\Delta F = 0.05$ and $\Delta F = 0.1$, the correct determination of the reactor's operational status is possible after a ≥ 4. Additionally, with an increase in '*a*', the *FDF* during a fault operation deviates further from the *FDF* during normal operation. Consequently, it becomes easier to determine the operational status of the reactor.

Table 3. The reactor parameters of BKGKL-20000/35.

Parameters	Value	Parameter	Value
Rated capacity (kVar)	20,000	Rated current (A)	989.7
Rated voltage (kV)	20.21	Height (mm)	2540
Number of encapsulates	14	Outer radius (mm)	3024
Number of coils	44	Equivalent reactance (Ω)	20.65
Rated frequency (Hz)	50	Equivalent resistance (Ω)	0.039

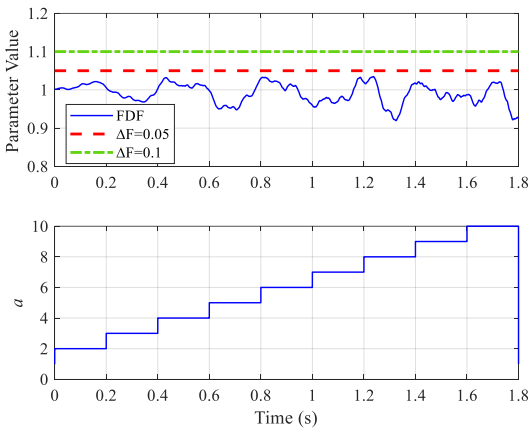

Figure 11. The fault factor curve handled by a moving average filter with the variation in exponent a when reactor II is under normal conditions.

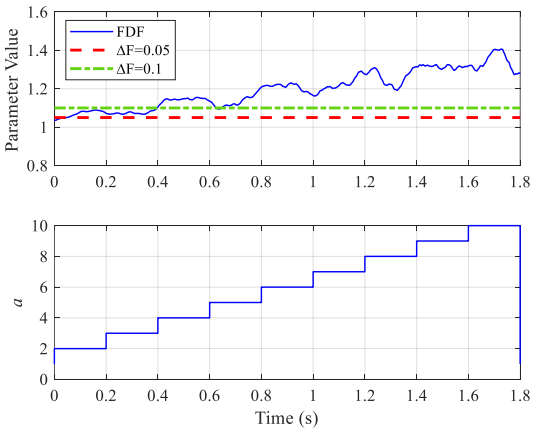

Figure 12. The fault factor curve handled by a moving average filter with the variation in exponent a when reactor II is under an inter-turn short-circuit fault condition.

4. Conclusions

In this paper, a new approach to detect an ISCF at the early stage of a dry-type air-core reactor is proposed, in which the *FDF* relies on equivalent resistance under normal

conditions and working conditions is introduced. To consider the effect of the noise signal measured during the condition monitoring, an MAF is adopted to improve the reliability and robustness of the *FDF*. The simulation results accounting for local ISCFs at an early stage highlight the promising potential of the proposed method, and the conclusions are as follows:

(1) For different coils within the same encapsulate of dry-type air-core reactors, the equivalent resistance and active power of a global ISCF at the same height show almost no change. As the fault moves outside the encapsulate, both the equivalent resistance and active power increase initially and then decrease. Moving from the middle to the end of the fault height results in a decreasing trend.
(2) The equivalent resistance and active power experience significant increments in the presence of an ISCF, reaching up to 50 and 60 times the rated values, respectively, without accounting for insulation resistance.
(3) At the initial stage of a local ISCF with one turn, the insulation resistance is relatively high, making it challenging to detect the fault. A larger exponent '*a*' in the FDF has better sensitivity in detecting ISCFs under the aforementioned condition without considering the noise signal.
(4) The *FDF* applied with an MAF can improve the reliability of the proposed method by reducing the fluctuation amplitude of the *FDF* to reduce the misjudgment likelihood in ISCF detection while guaranteeing the sensitivity of the detection proposed method when the signal noise in the monitoring system is considered.

This paper proposes a simple and sensitive way to detect ISCFs in dry-type air-core shunt reactors. The disadvantage of this work is that it is limited to verifying the method at a simulation level. The experimentation validation when the reactor is under an ISCF is a work in progress, and it will be completed in our future work.

Author Contributions: Conceptualization, J.W., W.Z. and Z.C.; methodology, J.W. and M.Z.; validation, M.Z. and Y.P.; formal analysis, W.Z. and Y.P.; investigation, Z.C.; data curation, Y.P., Y.L. and Q.H.; writing—original draft preparation, M.Z.; writing—review and editing, J.W., W.Z., Z.C., Y.P., Y.L. and Q.H. All authors have read and agreed to the published version of the manuscript.

Funding: This research was funded by State Grid Sichuan Electric Power Company scientific project, grant number 52199722000T.

Data Availability Statement: The data included in this article that support the results of this study can be obtained by contacting the corresponding author of this article.

Conflicts of Interest: Authors Jie Wu, Wei Zhen and Zhengwei Chang were employed by the company Electric Power Research Institute of State Grid Sichuan Electric Power Company. The remaining authors declare that the research was conducted in the absence of any commercial or financial relationships that could be construed as a potential conflict of interest. The authors declare that this study received funding from State Grid Sichuan Electric Power Company. The funder was not involved in the study design, collection, analysis, interpretation of data, the writing of this article or the decision to submit it for publication.

References

1. Sun, Y.; Zou, L.; Liu, Q.; Dai, L.; Zhang, L.; Zhao, T. Research on five-loop simplified scaling model for dry-type air-core reactors with inter-turn short circuit fault. *IEEE Access* **2021**, *9*, 163707–163715. [CrossRef]
2. Nie, H.; Liu, X.; Wang, Y.; Yao, Y.; Gu, Z.; Zhang, C. Breaking overvoltage of dry-type air-core shunt reactors and its cumulative effect on the interturn insulation. *IEEE Access* **2019**, *7*, 55707–55720. [CrossRef]
3. Das, S.; Sidhu, T.; Zadeh, M.D.; Zhang, Z. A novel hybrid differential algorithm for turn to turn fault detection in shunt reactors. *IEEE Trans. Power Deliv.* **2017**, *32*, 2537–2545. [CrossRef]
4. Vázquez, E.; Andrade, M.A.; Esponda, H.; Ávila, J. A new differential protection algorithm for power reactors based on the second central moment. *Electr. Power Energy Syst.* **2020**, *118*, 10579. [CrossRef]
5. Li, Y.Q. Operation analysis and operation and maintenance method of 35 kV dry-type air-core shunt reactor. *Electr. Eng.* **2018**, *18*, 39–40+53.

6. Jiang, J.Q.; Shi, W.F.; Liu, Y.H.; Xie, J.L. Early Warning of Interturn Short Circuit Fault of Stator Winding of Ship Generator. *CSU-EPSA*. [CrossRef]
7. Li, Q.; Wang, Z.; Zhao, H.B.; Dong, J.P.; Shen, Z.Y.; Zhang, X.Y.; Zhang, Z.; Hu, E.; Xing, Y. Interturn fault detection algorithm for shunt reactors based on leakage magnetic field. In Proceedings of the 2019 IEEE 3rd Conference on Energy Internet and Energy System Integration, Changsha, China, 8–10 November 2019. [CrossRef]
8. Zhou, D.Z.; Xv, M.K.; Du, X.M.; Fu, Z.Y.; Lv, X.P.; Kang, Q.K.; Song, H. Study for spatial magnetic field distribution of inter-turn short-circuit fault degree in dry air-core reactors. In Proceedings of the 2018 13th IEEE Conference on Industrial Electronics and Applications, Wuhan, China, 31 May 2018–2 June 2018. [CrossRef]
9. Tian, Y.F. Research of fault detection method of dry-type power reactor at substations. *South. Power Syst. Technol.* **2010**, *4* (Suppl. S1), 60–63. [CrossRef]
10. He, L.; Huang, Z. Fault diagnosis of dry-type air-core reactor based on temperature field with multi-component normal distributions. In Proceedings of the 2020 Chinese Control and Decision Conference, Hefei, China, 22–24 August 2020. [CrossRef]
11. Yang, H.; Lu, G.; Ji, S.; Zhu, L. Detection method of turn to turn insulation short circuit fault of dry-type air-core reactor using vibration characteristics based on machine learning. In Proceedings of the 2019 IEEE 8th International Conference on Advanced Power System Automation and Protection, Xi'an, China, 21–24 October 2019. [CrossRef]
12. Zhu, L.; Du, Y.; Gao, L.; Zhuang, Z.; Ji, S. Vibration Distribution Detection Method for Turn-to-Turn Short-Circuit Fault of Dry-Type Air-Core Filter Reactors. *IEEE Trans. Power Deliv.* **2022**, *37*, 4474–4476. [CrossRef]
13. Guo, Z.; Guo, Z.G.; Jia, G.M.; Lang, Q.; Liu, X.; Luo, F. Three-stage characteristic analysis on inter-turn fault and comprehensive protection method for air-core shun reactor. *Autom. Electr. Power Syst.* **2020**, *44*, 149–156. [CrossRef]
14. Gao, Z.W.; Zhu, X.C.; Wang, Y.H.; Zhuang, Y. Study on turn-to-turn short circuit on-line monitoring system for dry-type air-core reactor. *J. Harbin Univ. Sci. Technol.* **2017**, *22*, 67–71. [CrossRef]
15. He, L.; Zhengyi, H. Fault diagnosis of dry-type air-core reactor based on hierarchical neural networks. In Proceedings of the 2020 Chinese Control and Decision Conference, Hefei, China, 22–24 August 2020. [CrossRef]
16. Qin, R.S.; Wang, W.L.; Wang, B. Research on the modeling method and turn-to-turn short circuit monitoring method for the dry-type air-core reactor. In Proceedings of the 2018 2nd IEEE Conference on Energy Internet and Energy System Integration, Beijing, China, 20–22 October 2018. [CrossRef]
17. Li, N.; Zhang, X.; Yao, C.H.; Ran, B.; Mi, Y.; Cheng, J.C. Research on inter-turn short circuit fault detection method of dry-type air-core reactor based on IFRA magnetic coupling. *Electr. Eng.* **2022**, *15*, 83–87+91. [CrossRef]
18. Wang, J.; Zhang, G.Z.; Zhao, X.Z.; Zhang, L.; Liang, N.F.; Yao, C.G. Online detection investigation of the high voltage shunt reactor winding deformation based on coupling injection of pulses. *High Volt. Eng.* **2017**, *43*, 872–878. [CrossRef]
19. Zhuang, Y.; Wang, Y.; Zhang, Q. Study on turn-to-turn insulation fault condition monitoring method for dry-type air-core reactor. In Proceedings of the 2015 IEEE 11th International Conference on the Properties and Applications of Dielectric Materials, Sydney, Australia, 19–22 July 2015. [CrossRef]
20. Zhuang, Y.; Wang, Y. A monitoring method of inter-turn insulation fault for dry-type air-core shunt reactor. In Proceedings of the 2018 12th International Conference on the Properties and Applications of Dielectric Materials, Xi'an, China, 20–24 May 2018. [CrossRef]
21. Ma, C.; Zhang, B.; Yan, Z.; Li, J. Detection of metallic turn-turn short circuit of dry air core reactor based on digital twin current method. In Proceedings of the 2nd International Conference on Electronic Materials and Information Engineering, Hangzhou, China, 15–17 April 2022. [CrossRef]
22. Solak, K.; Mieske, F.; Schneider, S. Modeling and detection of turn-to-turn faults in shunt reactors. *IEEE Access* **2021**, *10*, 1386–1400. [CrossRef]
23. Zhu, Y.; Xue, Z.; Zhou, Y.; Hu, J.; Liu, J.; Li, Z. Research and application of on-line monitoring device for dry-type air-core reactor. In Proceedings of the 2019 IEEE International Conference on Electron Devices and Solid-State Circuits, Xi'an, China, 12–14 June 2019. [CrossRef]
24. Huang, S.P.; Aggarwal, A.; Strangas, E.G.; Li, K.; Niu, F.; Huang, X.Y. Robust stator winding fault detection in PMSMs with respect to current controller bandwidth. *IEEE Trans. Power Electron.* **2021**, *36*, 5032–5042. [CrossRef]
25. Moon, S.; Jeong, H.; Lee, H.; Sang, W.K. Interturn short fault diagnosis in a PMSM by voltage and current residual analysis with the faulty winding model. *IEEE Trans. Energy Convers.* **2018**, *33*, 190–198. [CrossRef]
26. Wu, J.; Luo, R.; Zhang, M.; Peng, Y.M.; Jing, S.; Huang, Q. A New Method to Detect the Inter-Turn Short Circuit Fault of Dry-Type Air-Core Shunt Reactor. In Proceedings of the 2022 4th International Conference on Power and Energy Technology, Xining, China, 28–31 July 2022. [CrossRef]
27. Zhao, C.M.; Wang, Y.H.; Ao, M.; Zhuang, Y. Electric parameter variation of dry-type air-core shunt reactor with interturn short-circuit fault. *Transformer* **2019**, *56*, 31–36. [CrossRef]
28. Chen, J.; Li, J.; Ge, N. Study on variation law of electrical parameters in dry hollow reactor inter-turn short circuit fault. In Proceedings of the IEEE International Conference on Properties and Applications of Dielectric Materials, Xi'an, China, 20–24 May 2018. [CrossRef]

29. Wei, X.L.; Zhu, B.; Nie, H.Y.; Yu, C.L.; Liang, J.Q.; Zhang, H.D. Relationship between electrical parameters and turn-to-turn insulation fault position of dry-type air-core reactor. *Electr. Mach. Control.* **2020**, *24*, 71–79. [CrossRef]
30. Zhu, B.J.; Liu, X.H.; Xie, T.P.; Xian, R.C.; Lu, Y.; Wang, L.Q. Analysis of electrical characteristics of series reactor winding inter-turn short-circuit fault. *Transformer* **2021**, *58*, 30–32. [CrossRef]